

LEVEL II

1

AD A090428

METHODOLOGY FOR EVALUATION OF OBSCURATION (U)

ELLIOT G. PETERSON, Mr
LOTHAR L. SALOMON, PhD
DUGWAY PROVING GROUND
DUGWAY, UT 84022

12/15

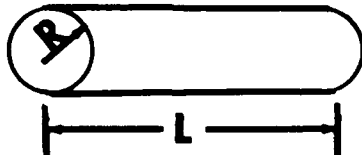
11/18

Since 1976, improvements in the methodology for physical and optical characterization of airborne obscurants have come about at a remarkable pace, reflecting the urgent need for objective data. Prior to that time virtually all evaluations of obscurants and associated delivery systems, and of electro-optical systems in an obscuring environment, were of the "go no-go" type. By contrast, a vast body of information is now available, much of which is based on developments at, and tests performed by Dugway Proving Ground. The purpose of this report is to describe some of the most recent advances in methodology.

A. SOURCE EMISSION RATE. A critical input to obscuration transport models is the source emission rate. It is defined as the fraction of mass burned as a function of time, i.e., $F_m(t) = (V_0 - V(t))/V_0$ (1), where V_0 is the volume of the submunition before burn, and $V(t)$ the volume at time t . The form of equation (1) was determined for five submunitions. The treatment leads to valid prediction of submunition performance, and should also be valuable in designing new submunitions.

Case 1. WP Wick Submunitions. A sketch of the wick submunition is shown in Figure 1.

Figure 1. Sketch of Wick Submunition



Using equation (1), the fraction of mass burned can be obtained using

$$F_m = 2\left(\frac{1}{L_0} + \frac{1}{R_0}\right)X - \left(\frac{4}{R_0 L_0} + \frac{1}{R_0^2}\right)X^2 + \left(\frac{2}{R_0^2 L_0}\right)X^3 \quad (2)$$

DDC FILE COPY

99

This document has been approved
for publication and its
distribution

118150
80 10 17 006

where L_0 is the length before burn, R_0 is the radius before burn, and X is the burn distance.

If the burn rate (dX/dt) is constant, the burn distance (X) is given by $X = X_b (t/t_b)$ (3), where X_b is the burn distance at burn-out and t_b is the burn time.

Using equations (2) and (3), the fraction of mass burned becomes

$$F_m = A(t/t_b) + B(t/t_b)^2 + C(t/t_b)^3 \quad (4)$$

where $A = 2(\frac{1}{L_0} + \frac{1}{R_0}) X_b$, $B = -(\frac{4}{R_0 L_0} + \frac{1}{R_0^2}) X_b^2$, and $C = (\frac{2}{R_0^2 L_0}) X_b^3$.

Table 1 is a list of theoretical constants used for three- and six-inch WP wicks.

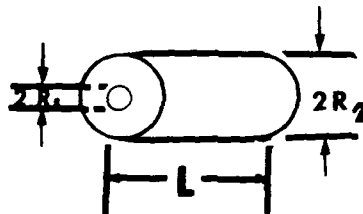
TABLE 1. Theoretical Mass Loss Constants

Type of Wick	R_0 (in)	L_0 (in)	X_b (in)	A	B	C
Three-Inch	0.5	3.0	0.5	2.17	-1.34	0.17
Six-Inch	0.5	6.0	0.5	2.33	-1.66	0.33

Equation (4) was used to calculate the theoretical fraction of mass burned as a function of time. The calculations are compared with experimental results (see Figures 2 and 3) and show good agreement for these two submunitions.

Case 2. 155 M1 (HC) Canister Submunition. A sketch of the 155 M1 (HC) canister is shown in Figure 4.

Figure 4. 155 M1 (HC)
Canister



It is assumed that the only surface burning is the center cylinder ($S = 2\pi R_1 L$) and the only parameter changing is R_1 . The fraction of the mass burned at any time becomes

$$F_m = \left(\frac{2R_{01}X_b}{R_2^2 - R_{01}^2} \right) (t/t_b) + \left(\frac{X_b^2}{R_2^2 - R_{01}^2} \right) (t/t_b)^2 \quad (5),$$

where R_{01} is the radius of R_1 before burn (0.681 in), R_2 is the outside radius (4.515 in) and the burn distance X_b is $R_2 - R_{01}$; and equation (5) then becomes

$F_m = 0.26(t/t_b) + 0.74 (t/t_b)^2$ (6). The comparison of equation (6) with experimental data is shown in Figure 5, and shows good agreement for the 155 M1 (HC) canister.

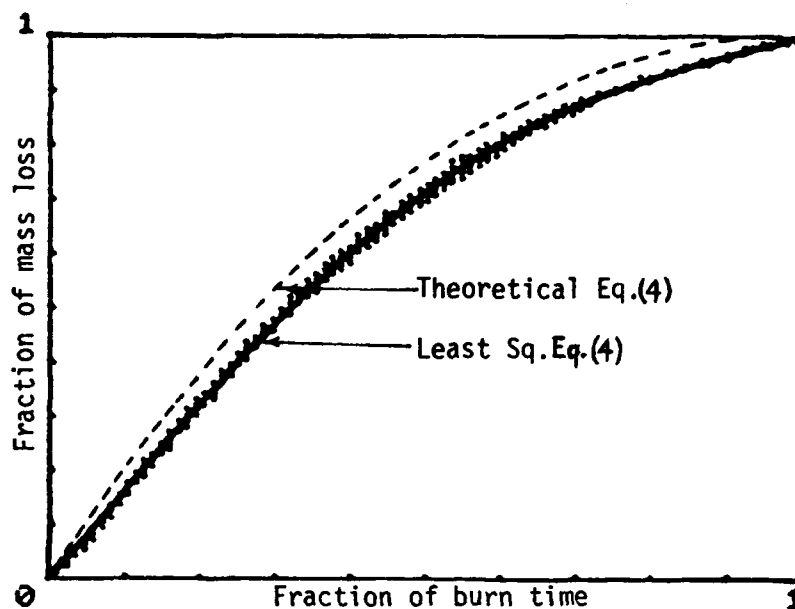


Figure 2. Three-Inch Wick (WP)

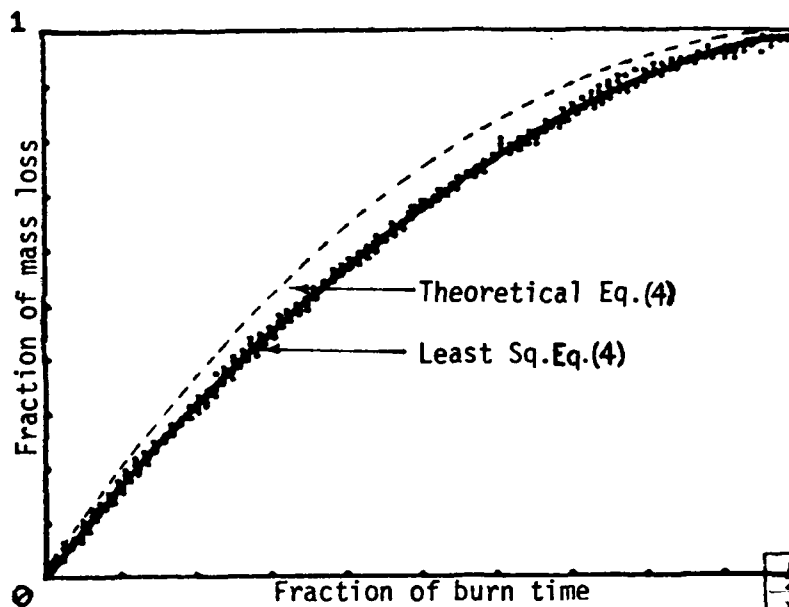
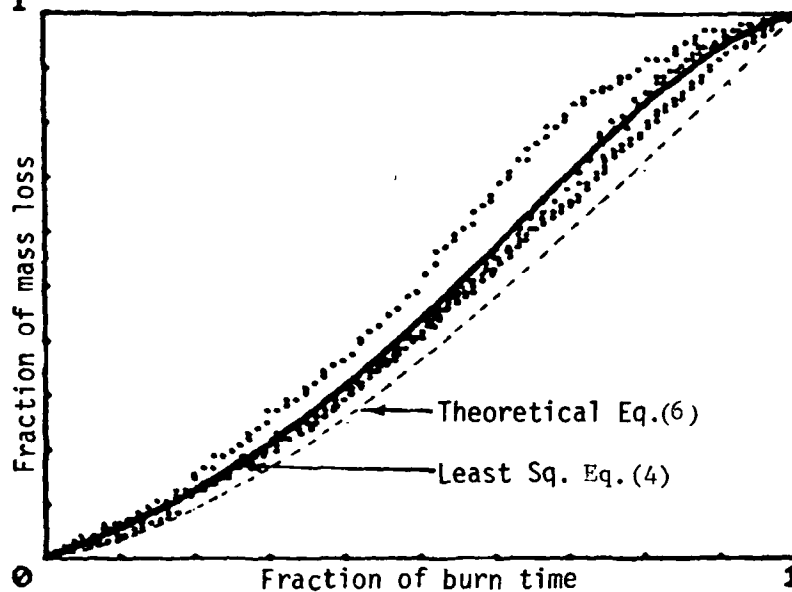


Figure 3. Six-Inch Wick (WP)

[illegible]

Figure 5. .155 mm Canister, M1, (HC)



Case 3. WP and RP Wedge Submunitions. Six wedges form a wafer shown in Figure 6.a; the wedge itself is shown in Figure 6.b.

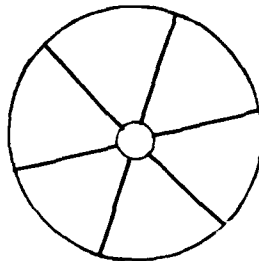


Figure 6.a

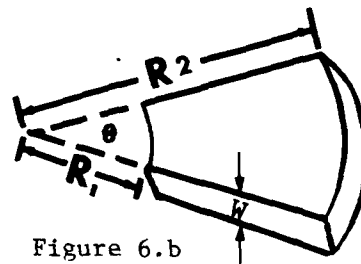


Figure 6.b

It is assumed that all surfaces burn. Equation (1) will then take the form of equation (4), where

$$A = 1 + \frac{W(aR_2 + bR_1)}{R_2^2 - R_1^2}, \quad B = -\frac{W[(aR_2 + bR_1) + (a^2 - b^2)\frac{W}{4}]}{R_2^2 - R_1^2},$$

$$C = \frac{W^2(a^2 - b^2)}{4(R_2^2 - R_1^2)}, \quad a = 1 + \frac{1}{\tan(\theta/2)}, \quad b = 1 - \frac{1}{\tan(\theta/2)}, \quad X_b = W/2$$

*PETERSON, SALOMON

Table 2 contains a list of theoretical constants used for WP and RP wedges.

TABLE 2. Theoretical Mass Loss Constants

Type	R_{01} (in)	R_{02} (in)	W (in)	θ (deg)	a	b	A	B	C
RP	0.375	2.375	0.50	30	2.732	0.732	1.62	-1.25	0.63
WP	0.375	2.375	0.75	30	2.732	0.732	1.92	-1.10	0.18

Equation (4), along with constants in Table 2, was used to calculate the theoretical fraction of mass burned as a function of time for WP and RP wedges. The calculations compare well with experimental results (see Figures 7 and 8).

B. RELATIVE HUMIDITY (RH) AND HYGROSCOPIC OBSCURANTS. Most of the conventional smokes, including those produced by burning of phosphorus and HC, are constituted of hygroscopic particles. It has been predicted, and established by field tests, that transmittance of phosphorus and HC smokes (i.e., their light-attenuating capability) can vary considerably with RH. In the Beer-Lambert Law $T = \exp(-\alpha CL)$, both α and C are potentially dependent on RH. (Here, T is transmittance (dimensionless), α is the extinction coefficient of smoke (m^2/g), C is the concentration of smoke (g/m^3), L is the thickness of the attenuating layer (m) along the line of sight, and t is time.) Thus α cannot be relied upon as an indicator of the light-attenuating characteristics of hygroscopic smokes. Indeed, we have found that α may remain virtually unaffected by changes in RH while T varied because of changes in C . By redefining α this ambiguity can be removed.

Transmittance of free-floating (unconfined) clouds can be determined using a modified form of the Beer-Lambert Law, $T = \exp(-\alpha' C_d L)$ (7). We recommend a new procedure for calculating transmittance by defining the extinction coefficient to be $(\alpha' = Y\alpha)$; equation (7) then becomes $T = \exp(-\alpha' C_d L)$ (8). Values of α' over the RH range and at the wavelengths of interest can then be determined using $\alpha' = -\int \ln T dt / \int C_d dL$ (9), where D_a is dosage ($\int C_d dt$), C_a is the concentration of smoke analyte which is independent of RH (e.g., phosphorus, zinc or, in general, $C_a Y = C$ smoke, g/m^3), and Y is a dimensionless yield factor which accounts for the difference in concentration between smoke analyte and actual smoke. For the hygroscopic phosphorus and HC smokes, analytes (C_a of equation (8)) are elemental phosphorus and zinc, respectively. Plots of α' at $3.4 \mu m$ wavelength are shown in Figure 9 as an example. For a non-hygroscopic smoke, α' versus RH would be constant.

In summary, once values of α' over the RH range and at wavelengths of interest have been determined, no further efforts are needed to

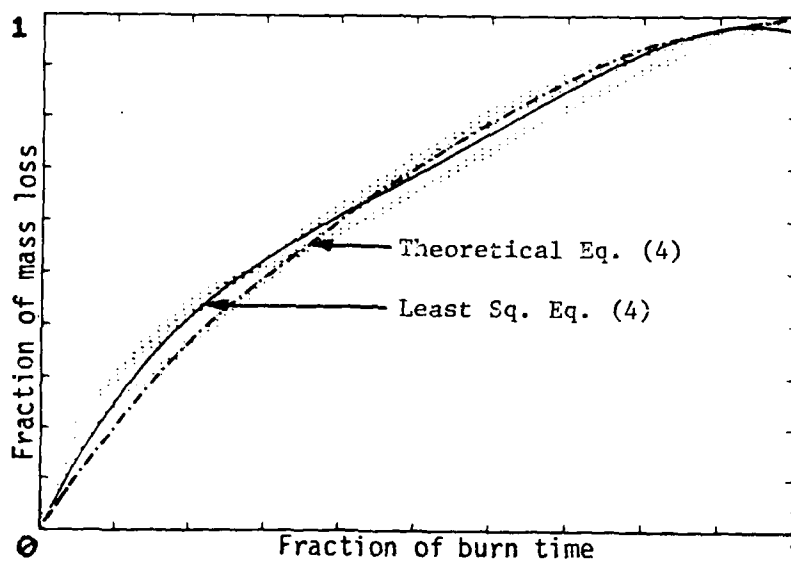


Figure 7. WP Wedge

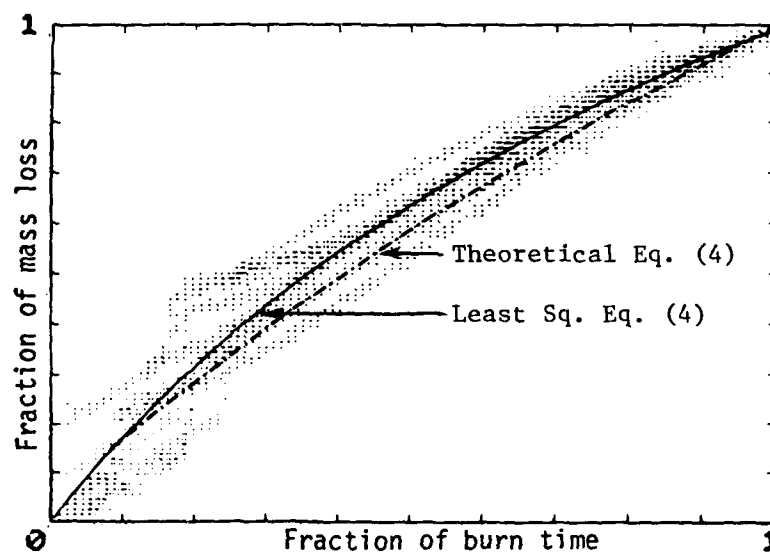


Figure 8. RP Wedge

ascertain yield factors, and most importantly, no assumptions are necessary regarding the chemical nature of the obscurants. (The fact that the composition of smokes varies with environmental conditions and, in many cases, remains uncertain, makes calculation of Y from literature data virtually impossible.) In the present approach, modified extinction coefficients (α') become an unequivocal measure of the light-attenuating characteristics of all types of obscurants, whether or not they are hygroscopic. Relevant data are available from past field tests. Furthermore, no additional burden is placed on mathematical modelers of obscuration since values of C_a are required in any event, and calculations of concentration of smoke (using tenuous yield factors) become unnecessary.

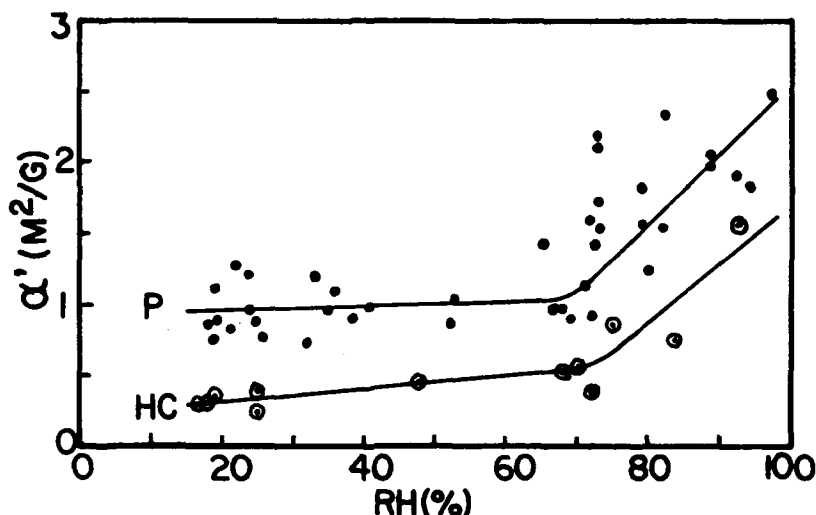


Figure 9. Extinction Coefficients α' ($\alpha Y, m^2/g$) for Phosphorus (P) and HC Smokes at 3.4 μm Wavelength from Field Data.

Coefficients vary little from about 17-70% RH: For phosphorus smokes, $\bar{\alpha}'_{3.4} = 0.97 \pm 0.19$ std. dev.; for HC smoke, $\bar{\alpha}'_{3.4} = 0.38 \pm 0.12$. However, beyond 70% RH, values increase rapidly. One consequence is that a required level of light attenuation can be achieved by greatly decreased munition expenditure. (Note that increases in α' are reflected by exponential decreases in transmittance.)

C. CORRELATION BETWEEN HUMAN VISION AND INSTRUMENTAL MEASUREMENTS.

Much emphasis is being placed on evaluating the effectiveness of modern military electro-optical devices in obscuring environments. On the battlefield, however, the human eye probably still is the most important sensor. It is, therefore, a question of practical consequence how instrumental measurements correlate with the ability of observers to spot a target. To explore this problem, trained observers with

7-power binoculars were required to record the time during which they were unable to see a stationary M48 tank through smoke clouds at 1000m or 1500m distance. (Perception of targets in realistic situations can involve a complex set of factors; not all were tested in this study.)

In Figure 10, the time during which the target was obscured to 5 observers at each of the two distances can be correlated with transmittance (T). It is immediately evident that less light attenuation is required for obscuration at the longer distance. However, the operation of complicating factors is seen in Table 3(I), because the T threshold for obscuration varies with type of munition despite adjustment for meteorological variables. In what follows, it will be seen that contrast ratios do not suffer from this defect. The contrast ratio through time is defined as $C_R(t) = [B_T(t) - B_B] / [B_B + B_C/T(t)]$, where T(t) is the visual transmittance through time, $B_C(t)$ is the luminance (visual) of the cloud through time, B_T is the luminance of the target as determined before cloud arrival, B_B is the luminance of the background as determined before cloud arrival. $C_R(t)$ takes account not only of light attenuation, but also the relative luminance of cloud, target and background. The $C_R(t)$ curve shown in Figure 11 and $C_R(t)$ threshold values seen in Table 3(II) demonstrate good correlation between measurements and observer responses, and reproducibility independent of transitory environmental effects such as sky brightness. By comparison with T, $C_R(t)$ clearly is a superior predictor of human response.

Table 3. Threshold Values for Transmittance and Contrast Ratios.

Round	(I) Ave Transmittance for Obscuration		(II) Ave Contrast Ratio for Obscuration	
	1000m	1500m	1000m	1500m
A(RP)	.0525	.109	.0075	.018
B(WP)	.019	.058	.0070	.019
C(HC)	.012	.042	.0075	.015
Mean/Std. Dev.	.0278/.0216	.0697/.0350	.0073/.0003	.0173/.0021

If one plots $C_R(t)$ against the time a munition can maintain a stated $|C_R|$ value or less, one can determine the obscuration effectiveness of the munition and its effectiveness relative to other munitions in the visual range. This is seen in Figure 12, which represents results from 15 trials with each of three types of 155mm smoke rounds, two of which are developmental types. The time during which each of the munitions provides a cloud dense enough to preclude detection of a target, that is, the time a cloud provides contrast ratios below the threshold for the eye, is indicated.

*PETERSON, SALOMON

TRIAL G4-C1, (SMK-001) 9 AUG 1978
HC 13:18:10

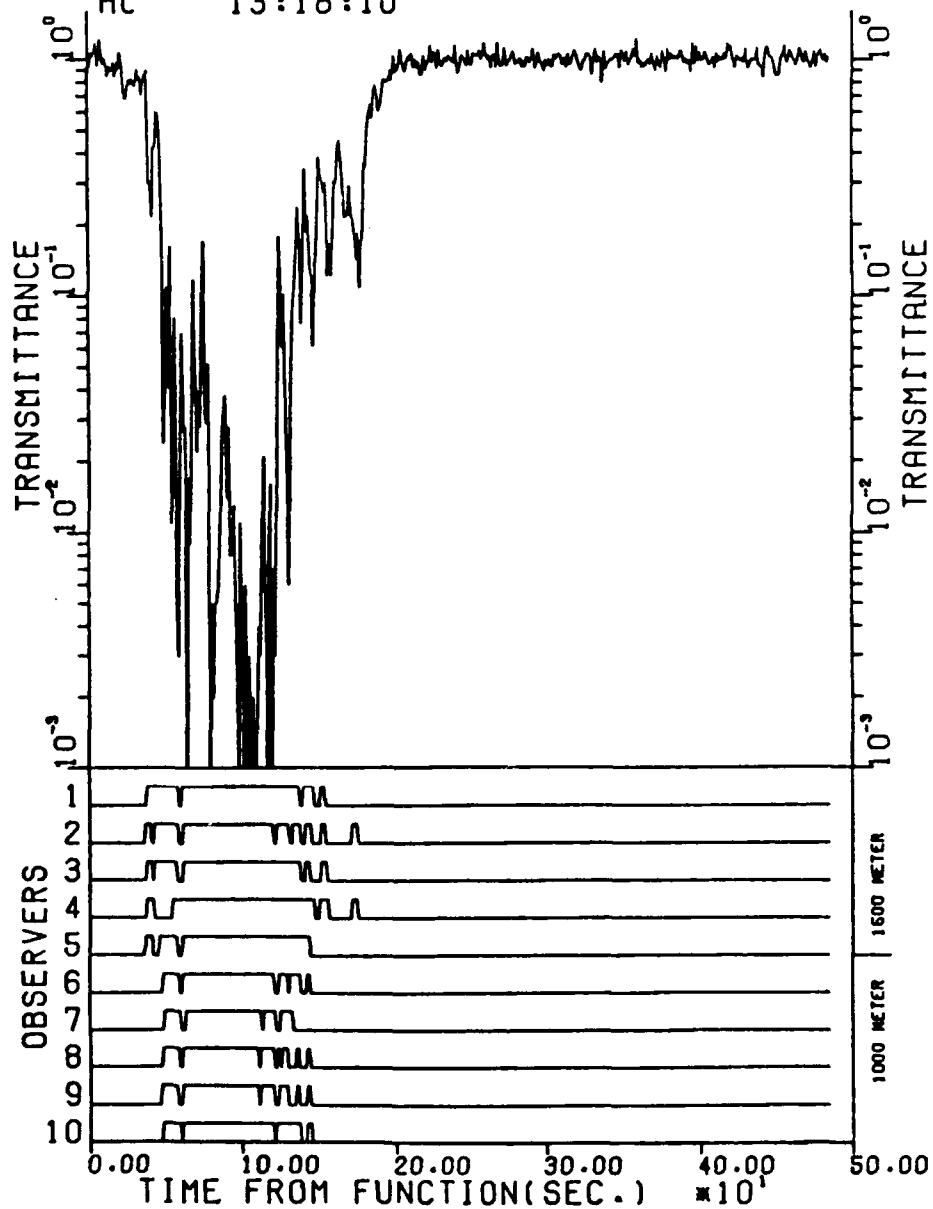


FIGURE 10. Transmittance and Observer Data Versus Time for Wavelength 0.4-0.7

(107)

*PETERSON, SALOMON

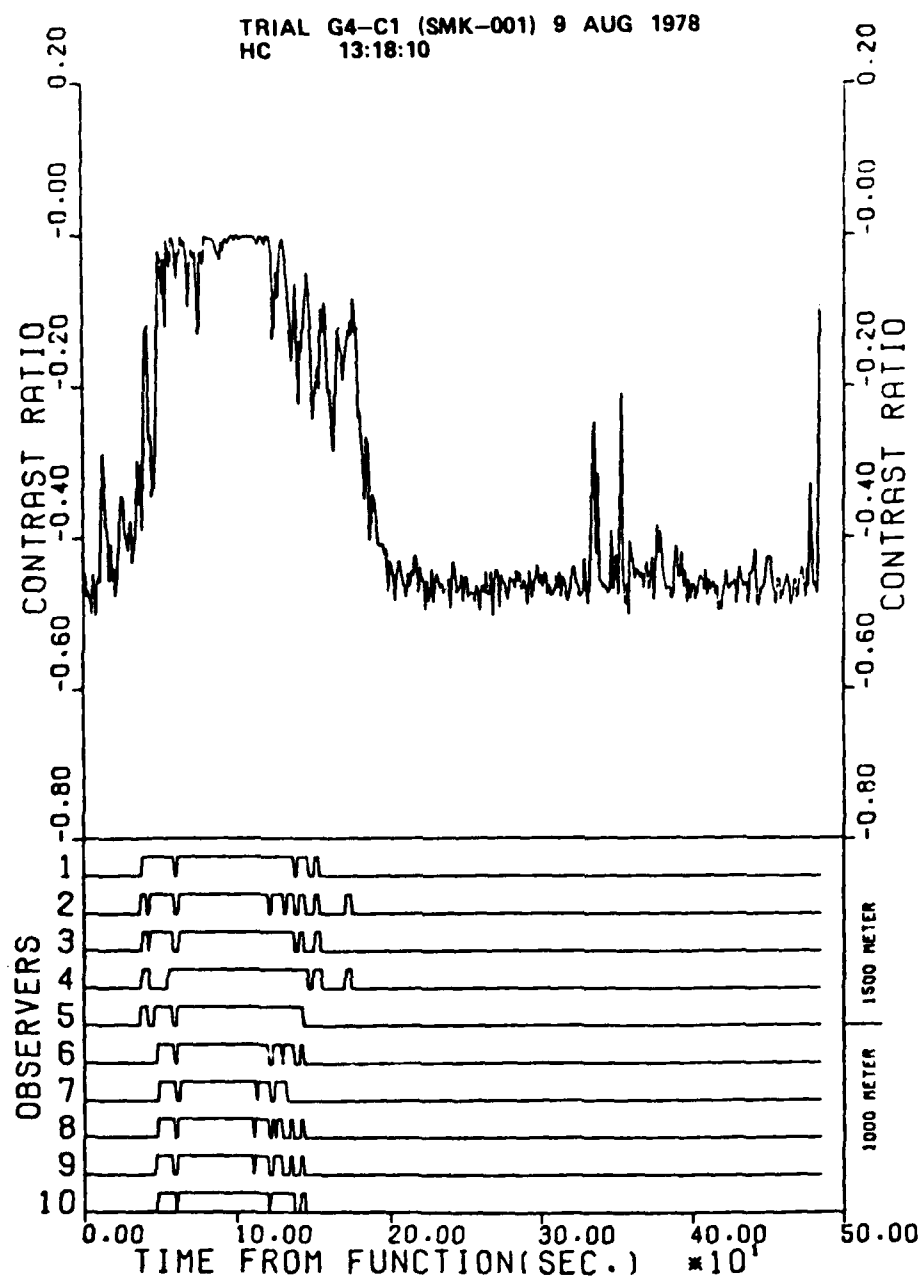


FIGURE 11. Contrast Ratio and Observer Data Versus Time for Wavelength 0.4-0.7

108

The significance of these findings is that objective instrumental measurements (a) correlate well with human responses, (b) can be used to predict the effectiveness of smoke rounds in obscuring vision, and (c) can be used in identifying munitions which provide obscuration of the required duration.

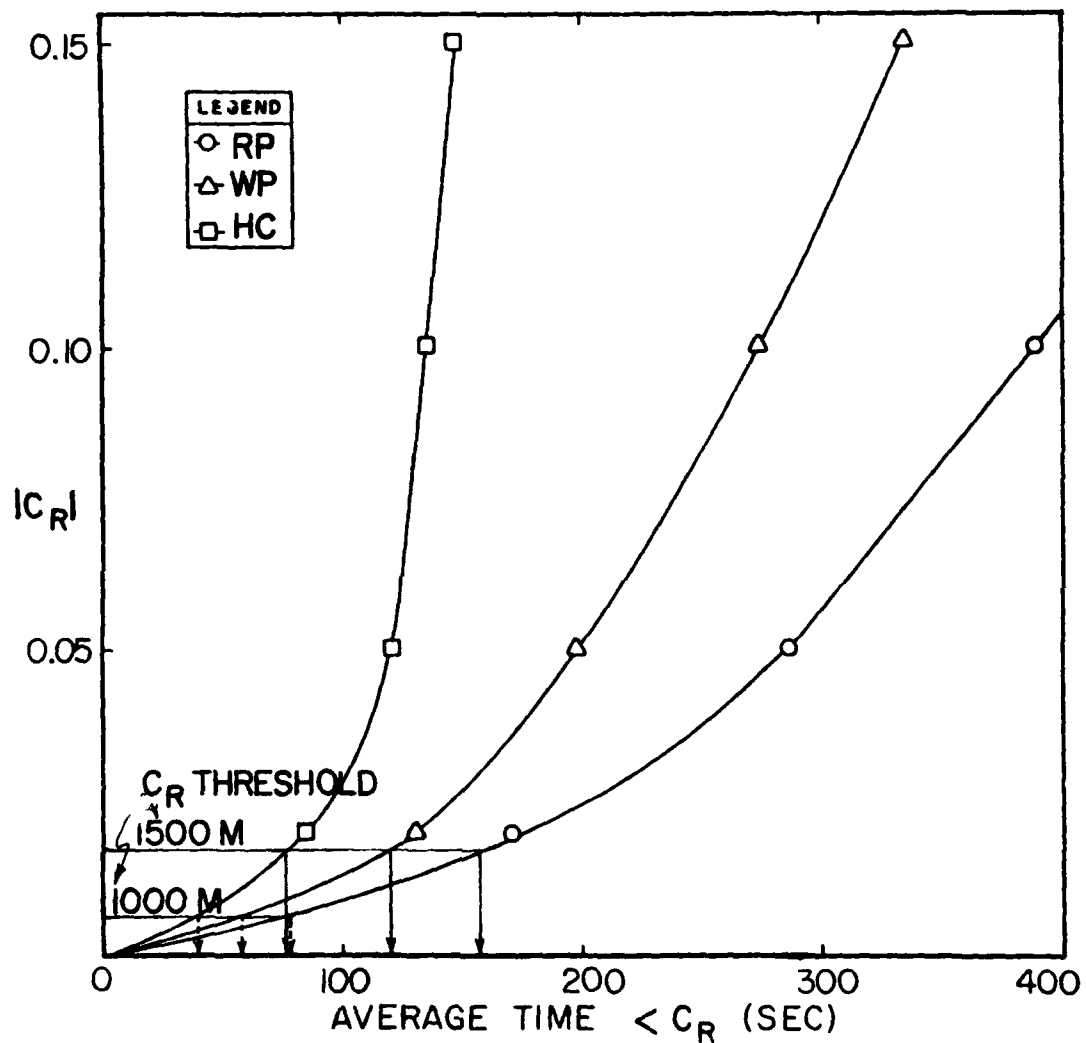


Figure 12. Time Contrast Ratio Remains below a Stated Level.

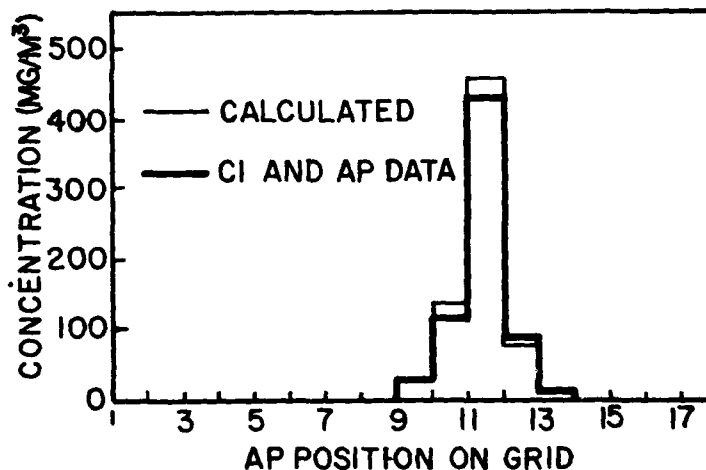
D. REAL TIME CONCENTRATION (C) AND CONCENTRATION-LENGTH PRODUCT (CL) VALUES. Aerosol photometers (APs) are routinely used by us to determine $C(t)$ of airborne obscurants. Involved in this procedure is the calibration of each AP using chemical impingers (CIs) which are positioned next to each AP during the field test. Since chemical analysis of CIs is relatively time-consuming, $C(t)$ cannot be computed until some time after the test day. To make $C(t)$ and $CL(t)$ values available in real time for test control and planning, the following automated method was developed and employed successfully.

Analog data from aerosol photometers are digitized and recorded on magnetic tape. In this form the data represent relative concentration through time. $CL(t)$ is defined as $\int C(t)dt = \sum A_i R_i(t) \Delta L_i$ (10), where A_i is the conversion factor from millivolts (mv) to concentration for the i -th AP, $R_i(t)$ is the reading of the aerosol photometer (mv) at time (t) and ΔL_i is the distance between APs. From the Beer-Lambert Law, $CL = \ln T / -\alpha$ (11). Let $Y = \ln T / -\alpha$ and $X = R \Delta L$. Then, in general, $Y = A_1 X_1 + A_2 X_2 + \dots + A_n X_n$ (12), and the conversion factors (A_i) can be obtained by a least square fit of equation (12) or

$$\begin{bmatrix} \sum X_1 X_1 & \sum X_1 X_2 & \dots & \sum X_1 X_n \\ \sum X_2 X_1 & \sum X_2 X_2 & \dots & \sum X_2 X_n \\ \vdots & \vdots & & \vdots \\ \sum X_n X_1 & \sum X_n X_2 & & \sum X_n X_n \end{bmatrix} \times \begin{bmatrix} A_1 \\ A_2 \\ \vdots \\ A_n \end{bmatrix} = \begin{bmatrix} \sum Y X_1 \\ \sum Y X_2 \\ \vdots \\ \sum Y X_n \end{bmatrix} \quad (12)$$

The APs are positioned along the same sampling line where the transmittance T is measured. The inputs to the least squares equation (12) at any given time t are $R_i(t)$, ΔL , α , $T(t)$ and repeated throughout time t at one-second intervals. Results of this method are shown in Figure 13 and show good agreement between the new method and the time-consuming method employing calibrated APs.

Figure 13.
Comparison between
Concentration Data
Obtained by Two
Methods (HC Smoke,
63 seconds after
Munition Function.)



(110)

*PETERSON, SALOMON

E. SUMMARY. In this report, we have presented descriptions and pertinent test data of selected methodological developments relating to evaluation (and, ultimately, weaponization) of obscuring systems.

It was shown that source emission rates for smoke submunitions can be predicted with substantial validity, thus providing a critical tool for mathematical modeling of obscuration and for the design of new submunitions with specified properties.

The relationship between transmittance and relative humidity was discussed for hydrated smokes, along with a demonstration of the drastic effect of high relative humidity on transmittance and its bearing on munition expenditure. A procedure was described for determination in the field of a redefined, unambiguous extinction coefficient which permits computation of transmittance without resort to yield factors, and is applicable to hygroscopic and non-hygroscopic smokes.

Evidence was presented which shows that instrumental measurements correlate well with human vision in assessing the obscuring properties of smokes. Applications to evaluation of smoke delivery systems were noted.

Finally, a mathematical treatment was described by means of which it becomes possible to obtain excellent estimates of concentrations through time, and concentration - length product time profiles, of obscuring clouds in real time, i.e., by a completely automated procedure. This is of particular value for field test control and test planning. Heretofore, such data were contingent on completion of chemical analysis of the contents of aerosol samplers, and thus unavailable for many hours or days.